ORIGINAL PAPER

Temporal changes in the spatial distribution of physicochemical properties during postharvest ripening of mango fruit

Busarakorn Mahayothee[1] · Parika Rungpichayapichet[2,3] · Pasinee Yuwanbun[1] · Pramote Khuwijitjaru[1] · Marcus Nagle[2,4] · Joachim Müller[2]

Abstract

While the temporal ripening behavior of mango is widely documented, the spatial distribution with respect to physicochemical composition remains largely unknown. In this study, ripening behavior of mangos cv. Nam Dokmai was investigated focusing on the variations between the different fruit parts, namely shoulder, cheek, and tip. The temporal results showed typical ripening behavior: color changes in pericarp and mesocarp with increase of a* and b* values and rises in total soluble solids (TSS) and pH, while firmness and titratable acidity (TA) decreased. Sucrose and citric acid were respectively the predominant sugar and acid in this particular cultivar. Relating to spatial variation, the shoulder (near the stem) had the highest TSS, pH, sugar to acid ratio (TSS·TA^{-1}), and sucrose, glucose, and fructose values. The tip showed the highest TA and citric acid content. Generally, the shoulder and tip were observed to ripen faster than cheeks. PCA was used to classify the ripeness of mango based on measured parameters and suggested that the cheek part is recommended for quality measurements. This information is imperative for the fruit handling industry, especially regarding the implementation of non-destructive technologies for quality determination.

Keywords Spatial variation · Fruit quality · Ripening behavior · Sugars · Organic acids

Introduction

Mango (*Mangifera indica* L.) is one of the most important fruit crops worldwide. Global production has continuously increased in recent years, reaching 50.6 million tons in 2017 [1]. Mango is preferred due to its unique taste, nutritional value, and attractive color as well as durability and suitable shelf-life. Since mango is a climacteric fruit which is commonly harvested at an unripe matured stage, its ripening process is a key step for proper utilization both as fresh and processed. The ripening process is performed at manufacture or packing house. In Southeast Asia, mango has been commercially ripened at an ambient temperature which is about 30–35 °C. Our previous study [2] showed that ripening at 33 ± 2 °C had more advantages than at 24 ± 2 °C not only in terms of lower operation costs but also higher β-carotene contents.

Mango and its products' market prices and customer satisfaction depend on fruit quality [3], which means that postharvest quality monitoring is essential to control and define fruit ripeness to achieve an increase in commercial value. Moreover, quality grading for maturity and ripeness allows for extension of shelf life and better classification of raw materials for different productions such as juice, dried mango and mango leather. However, mango ripeness can be complex to measure and understand since various parameters must be taken into consideration [4]. External quality attributes include uniform mass, color, and shape as well as lack of defects or damages [5]. The main internal attributes include firmness (F), mesocarp color, total soluble solids (TSS), titratable acidity (TA), pH, sugar-acid ratio

✉ Busarakorn Mahayothee
mahayothee_b@su.ac.th

1 Department of Food Technology, Faculty of Engineering and Industrial Technology, Silpakorn University, Nakhon Pathom 73000, Thailand

2 Institute of Agricultural Engineering, Tropics and Subtropics Group, Universität Hohenheim, Garbenstrasse 9, 70599 Stuttgart, Germany

3 Faculty of Agro-Industry, Panyapiwat Institute of Management, Nonthaburi 11120, Thailand

4 Agricultural Research and Development Program, Central State University, Wilberforce, OH 45384, USA

(TSS·TA^{-1}) and aromatic volatiles [5, 6]. These physicochemical properties are developed during both, fruit development (maturation) and ripening.

In producing countries, mango is generally sorted and graded by trained inspectors on a visual basis. In addition, destructive techniques are applied to measure internal characteristics of samples, providing results on mesocarp properties. However, such measurements must be done by representative sampling and thus cannot be applied to sort whole fruit lots, based on individual fruit characteristics. A variety of nondestructive methods have been applied for fruit quality determination [7, 8]. The uses of optical techniques, such as near-infrared spectroscopy [9–11] and computer vision [12–14] are established approaches to determine mango quality. Nonetheless, applications of these technologies are still limited since they are performed only externally or only on a limited part of the fruit, which decreases precision due to uneven distribution of the physicochemical properties [15]. For instance, Nordey et al. [16] found that the fruit tip of mango cv. Cogshall is sweeter and less acidic compared to the cheek and shoulder, and likewise, the shoulder flesh is more yellow than other parts. Ngamchuachit et al. [17] reported the physicochemical properties of cv. Tommy Atkins mango differed among fruit parts, specifically that the texture of the inner mesocarp (surrounding the endocarp) was softer than the outer mesocarp. Tissue at stem end position was found to be softer and redder-yellowish than the blossom end. Therefore, the aim of this study was to evaluate how the composition is distributed along fruits of cv. Nam Dokmai, also with respect to individual sugars and acids, as a basis for further development of nondestructive approaches that consider spatial variability in sorting and grading operations.

Materials and methods

Materials

Mature mango fruits cv. Nam Dokmai subcv. Si Thong were harvested from two planting areas of Thailand (Phitsanulok and Phetchabun provinces) at 120 days after full bloom. Mature fruits were identified according to specific gravity, where fruits that sink in water (density > 1.0 gcm^{-3}) were considered as fully mature. A total of 160 mature fruits were obtained, eighty from each production area at different periods. Fruit size and shape were also considered (mass ranging 291–350 g and diameter 57–63 mm) as well as the absence of any diseases or visual defects. Samples were transported to the laboratory in Nakhon Pathom province within 1 day where they were washed, air-dried and naturally ripened in baskets covered with paper at ambient temperature (32.0 ± 0.6 °C and 73.1 ± 6.6% relative humidity, RH).

Fruits were allowed to ripen for up to 8 days, with the first ripening day considered as the day samples were received. During experiments, ten fruits were randomly selected per day. Each of them was cut into three parts including shoulder, cheek and tip sections (Fig. 1) and the physicochemical properties were determined.

Fruit color and texture analysis

CIE L* a* b* values (L* for lightness, a* for redness and b* for yellowness) were determined using a HunterLab MiniScan XE Plus colorimeter (Hunter Lab, Reston, VA, USA). For pericarp color, data was directly obtained from the intact samples at each fruit position. The pericarp was then removed to a depth up to 1 mm, after which mesocarp color was determined at the same respective fruit positions. Measurements were done in triplicate for each position and the mean was used as absolute value. The color difference (ΔE) was calculated according to the following equation:

$$\Delta E = \sqrt{\left(L_2^* - L_1^*\right)^2 + \left(a_2^* - a_1^*\right)^2 + \left(b_2^* - b_1^*\right)^2} \quad (1)$$

where L_1^* a_1^* and b_1^* indicate color values on day 1 and L_2^* a_2^* and b_2^* represent color values on the respective ripening day.

Firmness of the mango was measured on one side of the fruit using the TA-XT2i Texture Analyser (Stable Micro Systems, Surrey, UK). A puncture test was carried out using a 2 mm diameter cylindrical probe at the cheek position with a speed of 0.5 mm s^{-1} and a compression depth of 10 mm. The maximum force (N) was recorded and used to describe the firmness.

Total soluble solids, pH value, and titratable acidity

Mesocarp samples from each fruit part were individually cut into small pieces and pulped using a homogenizer (Ultra-Turrax T25 basic, IKA Labortechnik, Staufen, Germany). Juice was extracted from 5 g of homogenized pulp and was

Fig. 1 Diagrammatic representation of mango sample and the respective positions taken for analyses
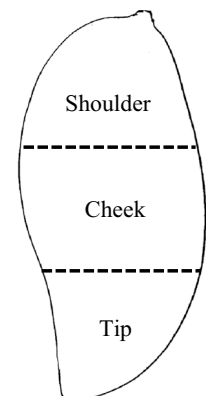
tested to determine total soluble solids content (TSS) using a digital refractometer (PAL-1, Atago, Tokyo, Japan). The pH was measured in 5 g of homogenized pulp using a pH-meter (Radiometer, PHM 210, Metro Lab, Villeurbanne, France). Titratable acidity (TA) was determined by titration with 0.1 mol L^{-1} NaOH until a pH of 8.1 was reached. Sugar-acid ratio (TSS·TA^{-1}) was calculated using TSS and TA values. Measurements were done in duplicate and the mean was used as absolute value.

Fruit ripeness classification

Ripening stage of mango was identified according to Rungpichayapichet et al. [10] using the ripeness index (RPI) which was introduced by Mahayothee et al. [2] and calculated from firmness, TA and TSS values as follows:

$$RPI = \ln (100 \ \cdot Firmness \ \cdot TA \ \cdot TSS^{-1}) \tag{2}$$

Quantitative analyses of individual sugars and organic acids

Homogenized pulp from each sample (2 g) was mixed with 8 mL of distilled water. The mixture was centrifuged at 9000 rpm for 15 min at 4 °C. The supernatant was filtrated through 0.45 μm nylon syringe filter and kept at − 18° for further HPLC analysis. Individual sugars, i.e. glucose, fructose and sucrose, were determined according to Liu et al. [18]. The HPLC system consists of a LC20AD pump, a CTO-10ASvp column oven, a CBM-20A system controller, and a refractive index detector (RID-10A, Shimadzu, Kyoto, Japan). Individual sugars were separated at 80 °C using a Rezex RCM-Monosaccharide Ca+2 column (7.8 i.d. × 300 mm, 5 μm particle size, Phenomenex, Torrance, USA), which was connected with a guard column. Deionized water was used as mobile phase with a flow rate of 0.6 mL min^{-1}. Calculations of glucose, fructose and sucrose were carried out using calibrations performed with certified standards (Sigma Aldrich, St. Louis, MO, USA). Results were expressed in g kg^{-1} edible part.

Quantitative analysis of six organic acids including: oxalic, malic, citric, succinic, tartaric and fumaric acids were performed using HPLC according to Liu et al. [18]. Separation of organic acid was achieved using a Luna 5 μm C18(2) 100A° column (4.6 i.d. × 250 mm, 5 μm particle size), which is equipped with a guard column at 30 °C. Mobile phases consisted of: A—0.01 mol L^{-1} potassium dihydrogen phosphate adjusted pH of 2.55 using orthophosphoric acid and B—100% methanol. Procedures were performed using an isocratic elution with 3% B and 97% A with a flow rate of 1 mL min^{-1}. Organic acids were detected using a photo diode array detector (SPD-20A, Shimadzu, Japan) at

210 nm. Certified standards of oxalic, malic, citric, and tartaric acids (Merck, Darmstadt, Germany) and also fumaric, malic, and succinic acids (Sigma-Aldrich, St. Louis, MO, USA) were used as calibration references. Results were expressed as g kg^{-1} edible part.

Statistical analysis

Analysis of variance (ANOVA) was performed using SPSS program (version 17, SPSS Inc., Chicago, IL, USA). Least significant difference (LSD) was used to test the significant differences between chemical compositions at each fruit position using ripening day as blocks. Principal component analysis (PCA) was employed to explore the correlation of the measured parameters and ripeness stages of mango. Fourteen parameters i.e. peel colors ($L*$, $a*$, $b*$, ΔE), flesh color ($L*$, $a*$, $b*$, ΔE), sucrose, glucose, fructose, and citric acid contents, TSS, and TA of 160 samples were used for the PCA analysis by R version 3.3.3. The data of each parameter were centered and scaled using *prcomp* function.

Results and discussion

Spatial variation of physicochemical properties within fruits during ripening

The overall pericarp color was observed to change considerably during ripening, i.e. decreasing L*, and increasing a*, b* and ΔE, with differences found for individual fruit positions, especially later in ripening (Fig. 2).

Rising a* values were clearly observed after 5 days of ripening. Pericarp color was found to be influenced by fruit position. For instance, lower L* and higher a* values were observed for shoulder than tip samples, meaning the shoulder was darker and more red. Non-significant differences of ΔE value within the fruit were detected at initial ripening stages (days 1–4). After that, the shoulder had the highest ΔE value, which implied the color difference was clearly attributed to the fruit ripening process [19]. However, changes in pericarp color during ripening of this cultivar could not be easily observed when compared to other green–red or green-yellow cultivars due to the effect of bagging treatments during production (i.e. covering the fruits with a paper bag during on-tree development) which tends to retard chlorophyll synthesis by preventing light exposure and cause enhanced development of pericarp color to golden yellow during ripening [20, 21].

Changes of mesocarp color parameters were more pronounced than the pericarp. Overall, a decrease in L* values and an increase of a*, b* and ΔE values were observed during ripening (Fig. 3). Loss of lightness (L*) was due to transformation of milky-green mesocarp color to
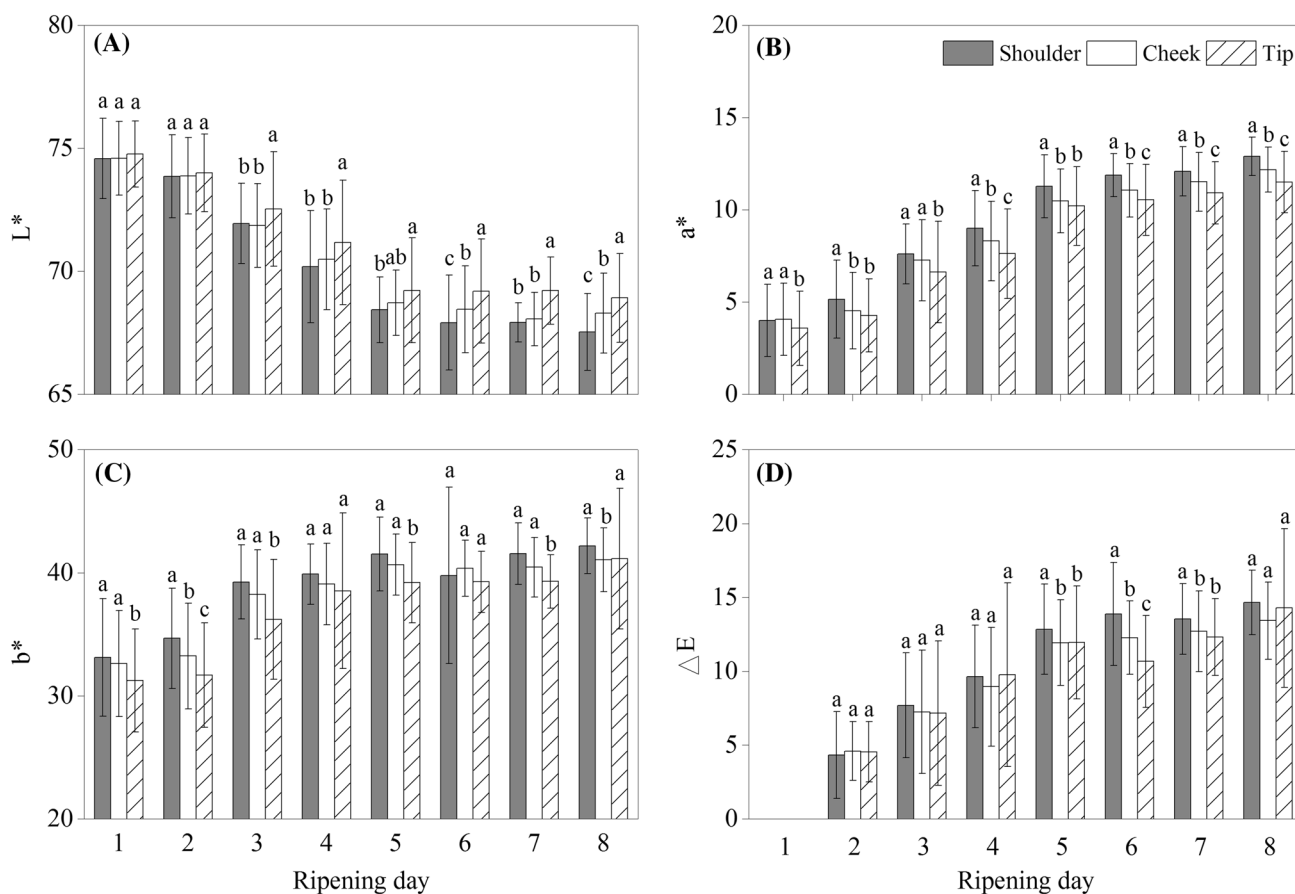
Fig. 2 Changes of L* (**a**), a* (**b**), b* (**c**) and ΔE (**d**) in pericarp color at different fruit positions during 8 days of ripening at 32.0 ± 0.6 °C and $73.1 \pm 6.6\%$ RH. Error bars show standard deviation. Same letters indicate no significant difference between fruit position ($P > 0.05$)

yellow-orange [19] influenced by the occurrence of enzymatic reactions during ripening [17]. Rapid increases of a* and b* values were detected over the days 1–4, which corresponded to chlorophyll degradation and carotenoid development [6, 9, 14]. Gradual rises in these parameters during ripening are generally a result of carotenoid biosynthesis [6]. The mesocarp color in tip had noticeably higher a*, b* and ΔE values than the shoulder. On the other hand, non-significant differences were found for L* values between those two parts, while the cheek presented the lowest L* value. Changing of mesocarp color in the shoulder and tip was more distinguishable than in the cheek, possibly due to the higher ethylene content at these positions.

Changes in chemical properties during ripening are depicted in Fig. 4. Typical ripening behavior was observed, namely increasing TSS, TSS·TA^{-1} and pH, while TA decreased. TSS had a range of 13.5–19.4°Brix from beginning to end of ripening. Substantial increases of TSS content were clearly seen in the period of days 1–3. After that, the values remained stable, and then tended to decline slightly during the end of ripening due to fruit senescence [22].

TSS accumulation is a result of increased activity of sucrose phosphate synthase and amylase during ripening, which hydrolyze starch into simple sugars (Fuchs et al. [23]; Castrillo et al. [27]). The cheek showed the lowest TSS content throughout the ripening process, while the highest value was conversely found at shoulder, however differences were not significant (Fig. 4a). This result is in disagreement with Nordey et al. [16] who found that the tip had higher TSS content due to the shorter distance between the pericarp and the endocarp, which allows for faster diffusion of ethylene. It is postulated that the lower TSS of the cheek in this study was due to the greater distance between the endocarp and the pericarp.

A sharp reduction in TA during the initial ripening phase was observed, which became relatively unchanged toward the end of ripening. TA varied widely from 1.60 to 16.4 g kg^{-1}. Compared to other cultivars, cv. Manila showed a higher reduction in TA (from 4.9 to 0.2%) while TA decrease in cv. Keitt variety was lower from 0.6 to 0.2% during a storage time of 14 days [6, 14]. Reduction of TA values resulted in increased pH from 2.96 to 5.65. Distributions of TA content and pH value within fruit are shown in
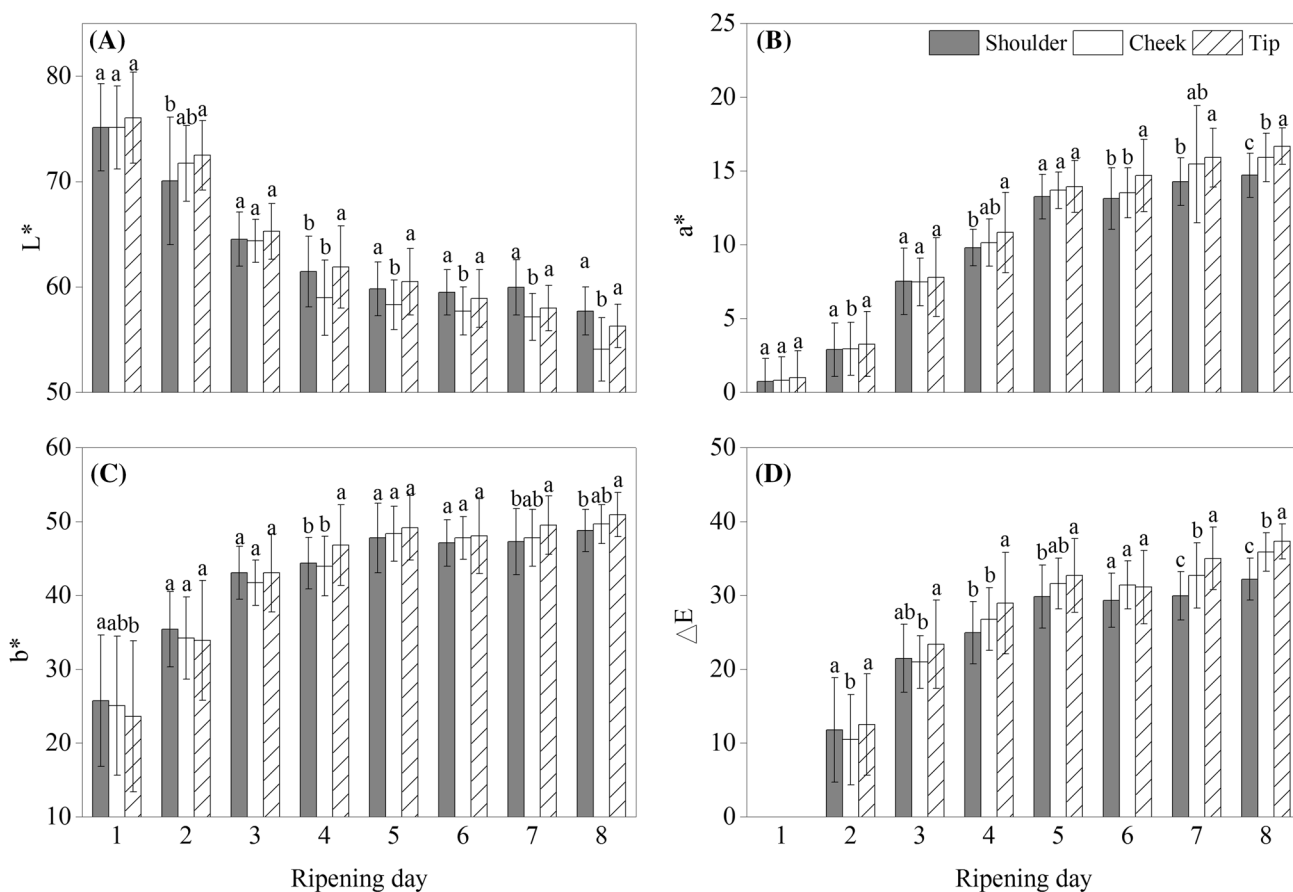
Fig. 3 Changes of L* (**a**), a* (**b**), b* (**c**) and ΔE (**d**) in mesocarp color at different fruit positions during 8 days of ripening at 32.0 ± 0.6 °C and $73.1 \pm 6.6\%$RH. Error bars show standard deviation. Same letters indicate no significant difference between fruit position ($P > 0.05$)

Fig. 4b and c, respectively. High variability of acidity was found between fruit positions, highlighted by the tip, which was significantly more acidic. The differences in acidity at several fruit positions were clearly observed during the initial phase of ripening and then diminished when the fruit completed ripening throughout the entire mesocarp. The results were in agreement with Nordey et al. [16] who found that quality traits of the mesocarp change in a gradient as the fruit ripens and TA experiences a maximum in the green mature fruits. The association between TA and pH values was also observed. Lower pH and higher TA were found in the tip, which suggested that the loss of TA occurred in parallel with the increase in pH.

TSS·TA^{-1} is the ratio of sweetness to sourness, indicative of the overall taste which impacts consumer acceptance. Results showed considerable increases in TSS·TA^{-1} after 5 days as a result of both increasing TSS and decreasing TA. Significant differences of TSS·TA^{-1} at several fruit positions were found throughout ripening (Fig. 4d). The shoulder had the highest TSS·TA^{-1} while the lowest was found in the tip. Based on this, ripening of the respective mango cultivar clearly started from shoulder and proceeded toward the tip.

The results correspond with studies by Jha et al. [7] and Ngamchuachit et al. [17] who reported that the ripening process ensues through proximal (shoulder) to distal end (tip) in fruits of other mango cultivars.

Ethylene is a plant hormone responsible for accelerating ripening and is initially introduced in the tissue close to the endocarp causing ripening from the core outwards. This phenomenon can also be seen in other climacteric fruits such as apples and bananas [24, 25]. Since there is less mesocarp tissue at the tip and shoulder of the fruit, ripening occurs faster in these areas. Interestingly, different anatomical factors such as stem scar, lenticels, and cuticle have been found to affect the exchange of volatiles which influence the accumulation and release of important compounds such as ethylene [26]. These volatiles may be respired differentially and thereby spatially impact the ripening process in fruits.

Spatial variation of individual sugars during ripening

Changes in individual and total sugars during ripening process are illustrated in Fig. 5. Sucrose was found to be the
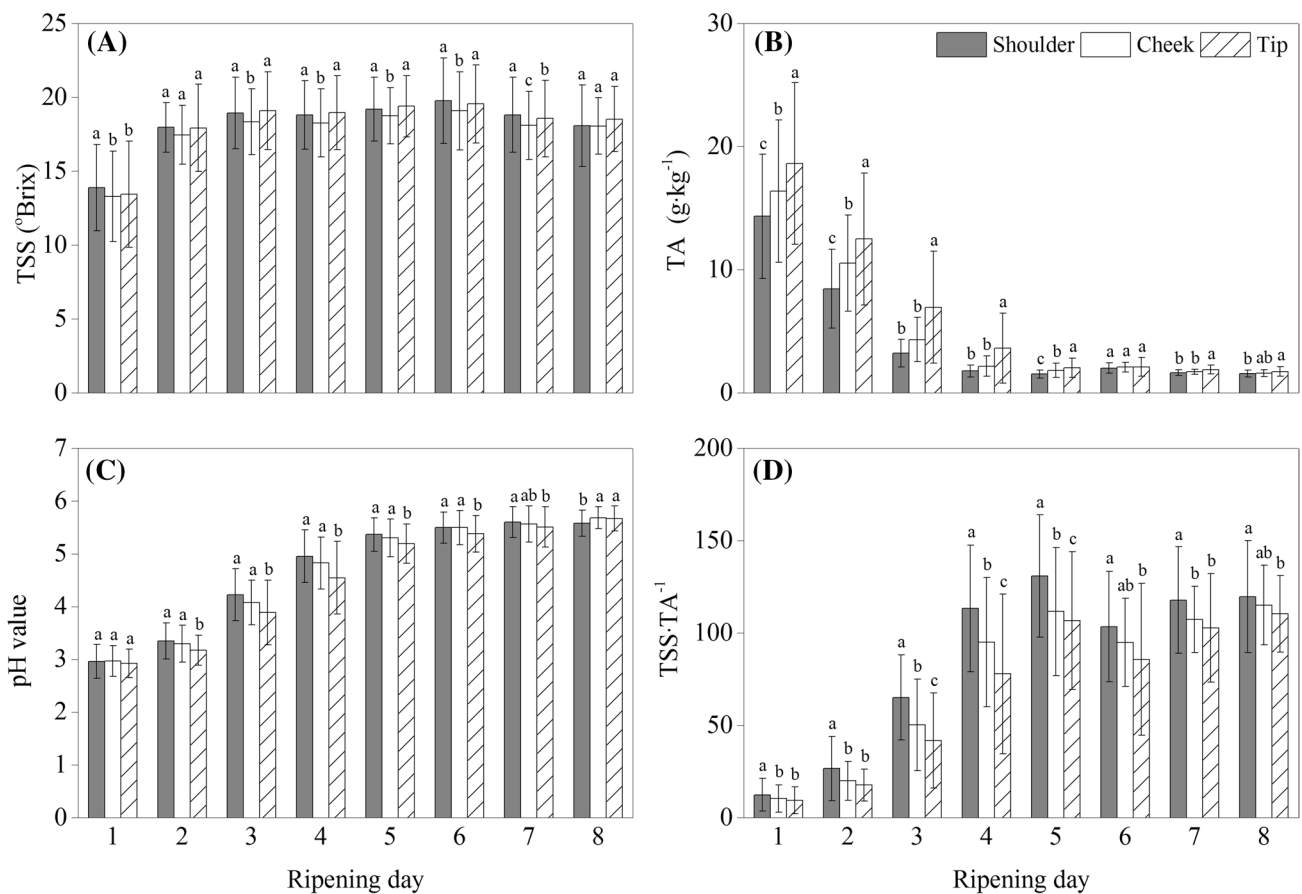
Fig. 4 Changes of TSS (**a**), TA (**b**), pH value (**c**) and TSS·TA^{-1} (**d**) content in mango at different fruit positions during 8 days of ripening at 32.0 ± 0.6 °C and 73.1 ± 6.6%RH. Error bars show standard deviation. Same letters indicate no significant difference between fruit position ($P > 0.05$)

predominant sugar throughout the ripening process with a range of 41.0–130.0 g kg^{-1} (41.3–76.0% of total sugar), followed by fructose (29.0–41.0 g kg^{-1}, 21.9–35.2% of total sugar), and glucose (3.0–14.0 g kg^{-1}, 2.2–15.5% of total sugar), respectively.

Similar compositions were found in other cultivars, i.e. 57% sucrose, 28% fructose, and 15% glucose was reported in cv. Keitt, whereas cv. Haden and cv. Tommy Atkins contain higher amounts of sucrose with more than 60 and 65% of total sugar content, respectively [18, 27, 28]. However, these results are inconsistent with other studies that reported fructose at a greater concentration in the initial phase of ripening [27, 29]. Rapid increases in sucrose content were clearly observed during days 1–4, with more gradual accumulation at the end of the ripening period.

Glucose and fructose both showed increases during the initial ripening stages (days 1–3), with subsequent declines toward the end of ripening. Fructose was found to be the main reducing sugar in this cultivar. Strong increases in fructose content were observed during days 1–2 with slight decreases after day 5. Decline of glucose content was

observed between days 4 and 5. With regard to the composition of sugars at each ripening stage, unripe fruits (day 1) showed sucrose/glucose/fructose (SGF) ratios around 4.9:1.6:3.5, while as the fruit ripened (day 4), the SGF ratio changed to 6.8:0.6:2.6. Escalations in the proportion of sucrose and declines of glucose and fructose content were further observed until the end of ripening (day 8) when the SGF ratio was at 7.8:0.2:2.0. Accumulation of sucrose is mainly due to the hexose phosphates synthesis via sucrose phosphate synthase accompanied with starch-sugar conversion [27, 29]. Reducing sugars were decreased by catabolic process since they are used as substrates during respiration [30].

Similar distribution patterns as seen for TSS were found for individual sugars and total sugars (Fig. 5), with the cheek generally showing the lower content. Interestingly, there were no clear trends in the sucrose content. In terms of fructose, the cheek was significantly lower in content than the shoulder and tip for most of the ripening process. Glucose content was also mostly lower in the cheek and strongly decreased overall halfway through the ripening period. The
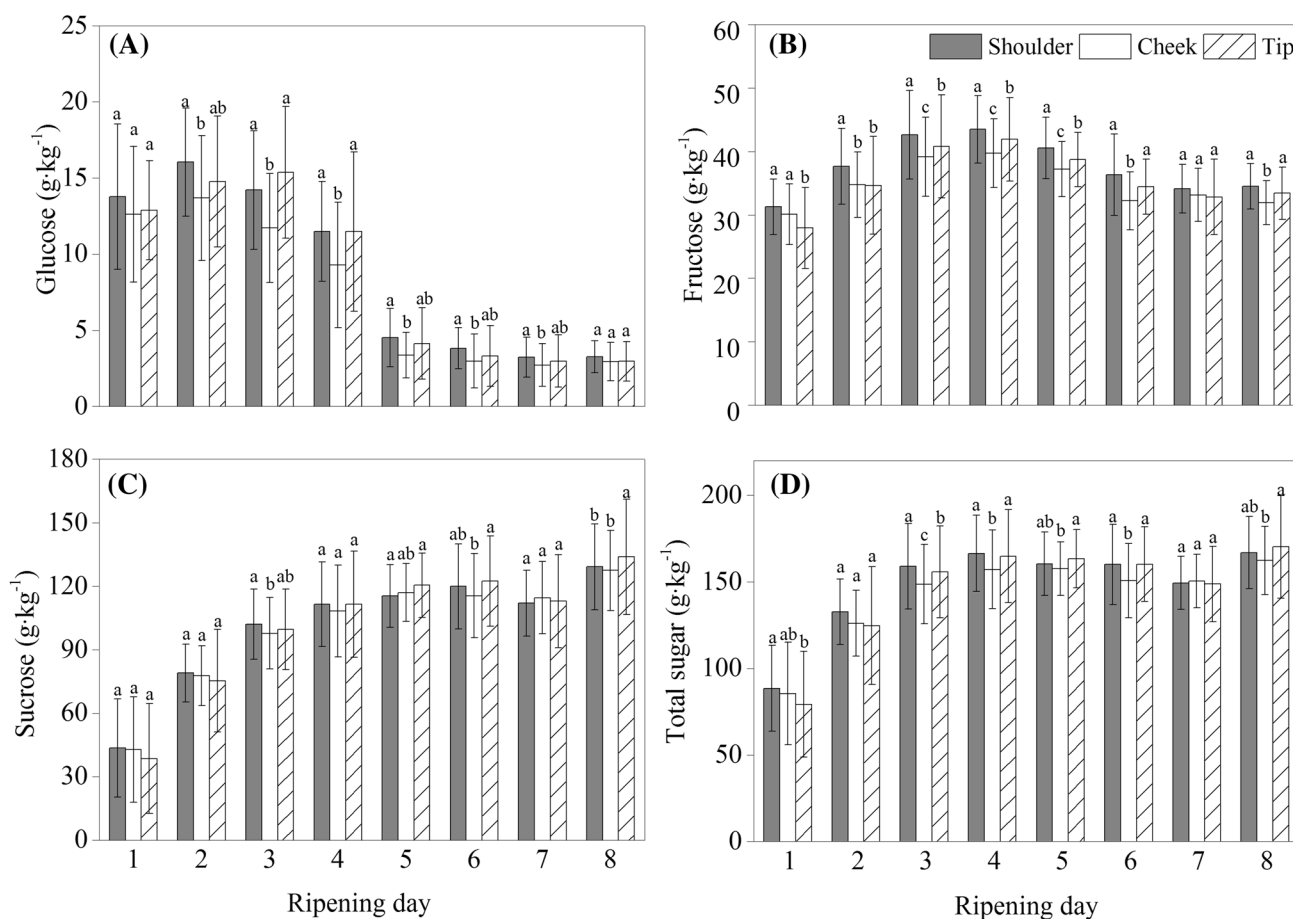
Fig. 5 Changes of glucose (**a**), fructose (**b**) and sucrose (**c**) and total sugar content (**d**) in mango during 8 days of ripening at 32.0 ± 0.6 °C and 73.1 ± 6.6%RH. Error bars show standard deviation. Same letters indicate no significant difference between fruit position ($P > 0.05$)

cheek exhibited the lowest sugar content throughout the ripening process, even though at the shoulder and tip were not always significantly different. Again, the pattern suggests the activity of sucrose phosphate synthase progress from the endocarp out through the mesocarp of the fruits as was observed in tomato (Wang et al. [31]).

Spatial variation of organic acids during ripening

A variety of organic acids produced during ripening and their distinctions in individual fruit parts are shown in Table 1. Content of organic acids generally tended to be higher in the tip of the fruit samples. Citric acid was the most predominant organic acid (ca. 45–92% of total organic acids), followed by succinic and malic acids. Since citric acid was most abundant, it showed a similar decreasing pattern to TA content. Results were consistent with Medlicott and Thompson [29] who reported that citric acid was the main organic acid in mango. Although, in some other cultivars i.e., cvs. Tainong No.1, Irwin, Jin Hwang and Keitt, formic acid has been reported as more abundant than citric acid

[18]. The different proportion of organic acids contribute to the overall characteristic taste properties in mango [32].

Rapid decrease of citric acid was observed during days 1–3 after which a more gradual reduction was observed (Table 1). Tartaric acid (ca. 3.63–12.03% of total organic acids) strongly declined over days 1–2 and then stabilized. A small amount of fumaric acid (ca. 0.03–2.95% of total organic acids) was found, which significantly increased later in ripening. Similar results were observed for oxalic acid (ca. 0.50–24.51% of total organic acids), which increased around five-fold over the ripening period. In contrast, malic and succinic acids showed no significant differences during ripening. Succinic and malic acid tended to decrease during the initial phase of ripening and later increased slightly in an indistinct pattern. The changes of tartaric acid were more pronounced at the cheek and tip than the shoulder, while citric acid modifications were more dominant at the shoulder. Fumaric acid clearly increased after 5 days and reached a maximum on day 8. Oxalic acid increase was distinctly observed during the ripening process and the tip showed less deviation than the other parts.

Table 1 Organic acid contents (g kg^{-1}) in different fruit parts during ripening at 32.0 ± 0.6 °C and 73.1 ± 6.6%RH

Ripening day	Citric acid			Succinic acid			Malic acid		
	Shoulder	Cheek	Tip	Shoulder	Cheek	Tip	Shoulder	Cheek	Tip
1	15.34 ± 5.94	18.32 ± 6.13	20.58 ± 6.87	1.66 ± 1.75	1.94 ± 1.74	1.68 ± 1.24	1.08 ± 0.33	0.88 ± 0.38	1.06 ± 0.41
2	9.52 ± 3.75	12.33 ± 5.08	12.08 ± 3.31	0.95 ± 0.80	1.45 ± 0.90	1.16 ± 0.69	0.40 ± 0.22	0.25 ± 0.19	0.54 ± 0.18
3	4.10 ± 2.05	5.83 ± 1.95	7.24 ± 2.74	1.03 ± 0.91	0.91 ± 0.98	0.95 ± 0.78	0.28 ± 0.18	0.13 ± 0.04	0.27 ± 0.16
4	1.71 ± 0.76	2.69 ± 1.06	3.82 ± 2.06	1.48 ± 1.17	1.12 ± 1.17	0.89 ± 0.78	0.25 ± 0.09	0.24 ± 0.10	0.25 ± 0.05
5	1.18 ± 0.87	1.93 ± 1.42	2.38 ± 2.17	0.55 ± 0.72	0.53 ± 0.48	0.41 ± 0.66	0.46 ± 0.13	0.40 ± 0.02	0.36 ± 0.00
6	0.82 ± 0.53	1.12 ± 0.45	1.23 ± 0.73	0.86 ± 0.97	0.35 ± 0.39	0.30 ± 0.15	0.68 ± 0.18	0.70 ± 0.09	0.79 ± 0.07
7	0.72 ± 0.34	1.15 ± 0.62	1.13 ± 0.63	1.03 ± 0.95	1.12 ± 0.53	0.89 ± 0.43	ND	ND	ND
8	0.84 ± 0.86	1.05 ± 0.48	0.90 ± 0.50	1.22 ± 1.12	1.53 ± 0.32	1.04 ± 0.83	ND	ND	ND

Ripening day	Oxalic acid			Tartaric acid			Fumaric acid		
	Shoulder	Cheek	Tip	Shoulder	Cheek	Tip	Shoulder	Cheek	Tip
1	0.09 ± 0.11	0.08 ± 0.14	0.13 ± 0.22	0.59 ± 0.41	0.72 ± 0.47	0.85 ± 0.38	0.01 ± 0.00	0.01 ± 0.00	0.01 ± 0.00
2	0.16 ± 0.23	0.13 ± 0.15	0.12 ± 0.15	0.25 ± 0.19	0.24 ± 0.16	0.27 ± 0.22	0.00 ± 0.00	0.00 ± 0.00	0.00 ± 0.00
3	0.22 ± 0.24	0.20 ± 0.23	0.17 ± 0.22	0.15 ± 0.05	0.16 ± 0.08	0.19 ± 0.08	0.00 ± 0.00	0.00 ± 0.00	0.00 ± 0.00
4	0.33 ± 0.32	0.29 ± 0.28	0.31 ± 0.30	0.24 ± 0.09	0.22 ± 0.06	0.26 ± 0.07	0.01 ± 0.01	0.01 ± 0.01	0.01 ± 0.01
5	0.38 ± 0.36	0.38 ± 0.34	0.39 ± 0.36	0.32 ± 0.14	0.25 ± 0.06	0.25 ± 0.04	0.02 ± 0.01	0.02 ± 0.01	0.02 ± 0.01
6	0.45 ± 0.48	0.40 ± 0.40	0.51 ± 0.50	0.25 ± 0.06	0.21 ± 0.06	0.24 ± 0.07	0.03 ± 0.03	0.03 ± 0.02	0.03 ± 0.02
7	0.31 ± 0.42	0.44 ± 0.37	0.45 ± 0.50	0.25 ± 0.06	0.22 ± 0.05	0.28 ± 0.07	0.03 ± 0.03	0.04 ± 0.03	0.04 ± 0.03
8	0.50 ± 0.50	0.47 ± 0.45	0.52 ± 0.57	0.27 ± 0.10	0.22 ± 0.05	0.26 ± 0.06	0.05 ± 0.04	0.06 ± 0.03	0.07 ± 0.04

ND not detected

Organic acid changes during ripening were associated with Krebs cycle reactions. Catabolism of citric acid during ripening occurs readily as it is a substrate in the Krebs cycle, besides from being converted to sugars by gluconeogenesis [28, 33–35]. Tavar et al. [36] reported that decrease of malic acid may be due to its use as malic enzyme for producing carbon dioxide, NADH, and pyruvate which are substrates for the Krebs cycle, while succinic acid is used as substrate to generate fumaric and malic acids. Malic and succinic acid variations during ripening could have also related to the enzymatic activity of malic and succinic dehydrogenase. Brecht and Yahia [37] reported that the high activity of malic and succinic dehydrogenase were found during the onset of ripening and later declined, which caused the malic acid and succinic acid reductions at the ripening initial phase.

Principal component analysis of data

Principal component analysis (PCA) was used to separate all mangoes into 4 ripening stages by the ripening index (RPI) which has been calculated from firmness, TA and TSS values as proposed by Mahayothee et al. [2]. According to the RPI values, the mangos could be classified into 4 ripening stages i.e. unripe (RPI > 5), half-ripe (RPI 4–5), ripe (RPI 2–4) and overripe (RPI < 2) as suggested by Rungpichayapichet et al. [10]. Based on this classification,

unripe mangos were found on the 1st day of ripening and half-ripe mangos were observed after ripening for 2 days. Ripe mangos, a major group of the sample in this study, were noticed after 3–6 days of ripening while the mangos from the last 2 days of ripening were mostly classified as overripe. The Pearson correlation coefficients between parameters that were not used in RPI calculation with the RPI values indicated high positive values (0.67–0.94) for L* of both peel and flesh parts, glucose and citric acid contents and negative values [− 0.67–(− 0.90)] for a*, b*, and ΔE of both peel and flesh parts and sucrose content.

Fructose content showed low correlation coefficients [− 0.25–(− 0.37)] with the RPI and was also insignificantly correlated with other variables, and therefore fructose content was not included in PCA determination. Figure 6 shows scores plot of the first two principal components (PC1 and PC2) using data from each mango part (shoulder, cheek, and tip). PC1 and PC2 explained about 82–85% of the total variance. From the result, it can be observed that unripe and half-life mangoes were clearly discriminated from the others while overripe and ripe mangoes could not be completely separated. Nevertheless, it was found that the data from cheek part tended to give a better discriminating result than shoulder and tip parts, therefore measuring ripeness of mango at the cheek part might give more accurate result.
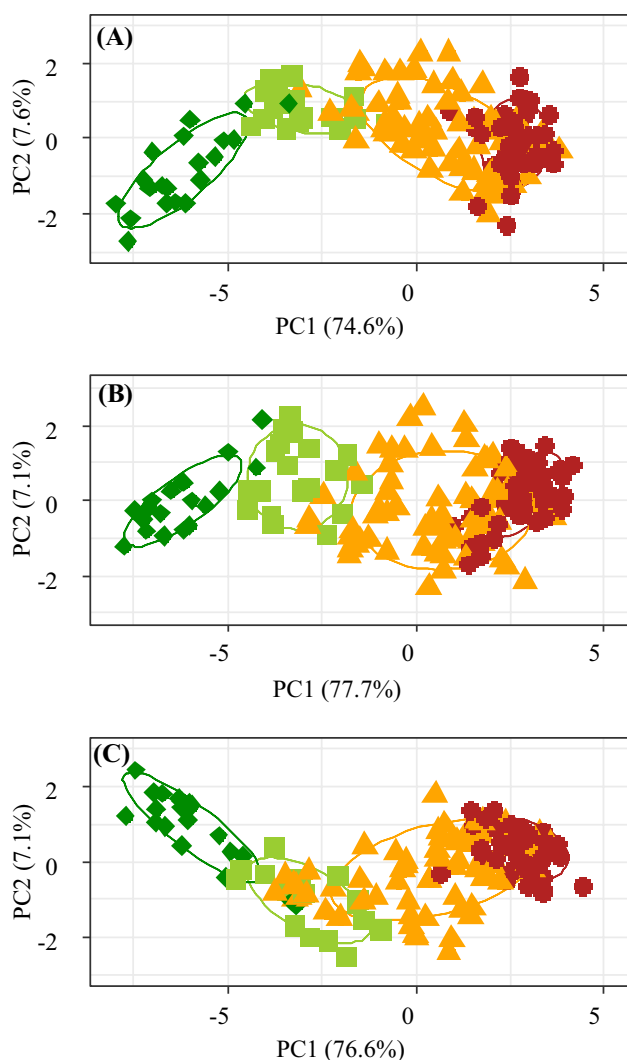
Fig. 6 Score plots for the mangoes at different ripening stages: unripe (filled diamond), half-ripe (filled square), ripe (filled triangle) and overripe (filled circle) using the data from shoulder (**a**), cheek (**b**) and tip (**c**)

Conclusion

The spatial variations of physicochemical properties within mango fruit cv. Nam Dokmai Si Thong during ripening were documented in this study. Fructose was found to be not significantly related to the ripeness of this cultivar. The results supported that the ripening process starts from the inner mesocarp near the endocarp and progresses to the outer mesocarp near the pericarp of the fruit. This causes variability in the tissue composition of the outer mesocarp, which has implications for point measurements of fruit quality like the widely-applied technique of near-infrared spectroscopy (NIRS). The prediction capability of NIRS calibrations, especially when small areas of sample are scanned to obtain the optical data, could be highly influenced by this

phenomenon. Therefore, cheek part is recommended for quality measurements.

References

1. FAO, FAOSTAT, Rome, Italy, 2019. http://www.fao.org/faostat
2. B. Mahayothee, S. Neidhart, R. Carle, W. Mühlbauer, Effects of variety, ripening condition and ripening stage on the quality of sulphite-free dried mango slices. Eur. Food Res. Technol. **225**, 723–732 (2007)
3. R.M. Salinas-Hernández, G.A. González-Aguilar, M.E. Tiznado-Hernández, Utilization of physicochemical variables developed from changes in sensory attributes and consumer acceptability to predict the shelf life of fresh-cut mango fruit. J. Food Sci. Technol. **52**, 63–77 (2015)
4. S. Kienzle, P. Sruamsiri, R. Carle, S. Sirisakulwat, W. Spreer, S. Neidhart, Harvest maturity detection for 'Nam Dokmai#4' mango fruit (*Mangifera indica* L) in consideration of long supply chains. Postharvest Biol. Technol. **72**, 64–75 (2012)
5. D. Sivakumar, Y. Jian, E. Yahia, Maintaining mango (*Mangifera indica* L.) fruit quality during the export chain. Food Res. Int. **44**, 1254–1263 (2011)
6. M. Padda, C. do Amarante, R. Garcia, D. Slaughter, E. Mitcham, Methods to analyze physico-chemical changes during mango ripening: a multivariated approach. Postharvest Biol. Technol. **62**, 267–274 (2011)
7. S.N. Jha, K. Narsaiah, A.D. Sharma, M. Singh, S. Bansal, R. Kumar, Quality parameters of mango and potential of non-destructive techniques for their measurement—a review. J. Food Sci. Technol. **47**, 1–14 (2010)
8. J. Li, D. Sun, J. Cheng, Recent advances in nondestructive analytical techniques for determining the total soluble solids in fruits: a review. Compr. Rev. Food Sci. Food Saf. **15**, 897–911 (2016)
9. P. Rungpichayapichet, B. Mahayothee, P. Khuwijitjaru, M. Nagle, J. Müller, Non-destructive determination of β-carotene content in mango by near-infrared spectroscopy compared with colorimetric measurements. J. Food Compos. Anal. **38**, 32–41 (2015)
10. P. Rungpichayapichet, B. Mahayothee, M. Nagle, P. Khuwijitjaru, J. Müller, Robust NIRS models for non-destructive prediction of postharvest fruit ripeness and quality in mango. Postharvest Biol. Technol. **111**, 31–40 (2016)
11. N. Wang, D. Sun, Y. Yang, H. Pu, Z. Zhu, Recent advances in the application of hyperspectral imaging for evaluation fruit quality. Food Anal. Method. **9**, 178–191 (2016)
12. M. Nagle, K. Intani, G. Romano, B. Mahayothee, V. Sardsud, J. Müller, Determination of surface color of 'all yellow' mango cultivars using computer vision. Int. J. Agric. Biol. Eng. **9**, 42–50 (2016)
13. K. Schulze, M. Nagle, W. Spreer, B. Mahayothee, J. Müller, Development and assessment of different modeling approaches for size-mass estimation of mango fruits (*Mangifera indica* L, cv.'Nam Dokmai'). Comput. Electron. Agric. **114**, 269–276 (2015)

14. N. Vélez-Rivera, N. Blasco, J. Chanona-Pérez, G. Calderón-Domínguez, M. de Jesús Perea-Flores, I. Arzate-Vázquez, S. Cubero, R. Farrera-Rebollo, Computer vision system applied to classification of Manila mangoes during ripening process. Food Bioprocess Technol. **7**, 1183–1194 (2014)

15. K.H.S. Peiris, G.G. Dull, R.G. Leffler, S.J. Kays, Spatial variability of soluble solids or dry-matter content within individual fruits, bulbs, or tubers: implications for the development and use of nir spectrometric techniques. HortScience **34**, 114–118 (1999)

16. T. Nordey, M. Léchaudel, M. Génard, J. Joas, Spatial and temporal variations in mango colour, acidity, and sweetness in relation to temperature and ethylene gradients within the fruit. J. Plant Physiol. **171**, 1555–1563 (2014)

17. P. Ngamchuachit, E. Mitcham, D. Barrett, Spatial variance of physicochemical properties within mangos and the effect of initial ripeness stage on the quality of fresh-cut mangos. J. Sci. Food Agric. **96**, 3613–3620 (2016)

18. F. Liu, S. Fu, X. Bi, F. Chen, X. Liao, X. Hu, J. Wu, Physicochemical and antioxidant properties of four mango (*Mangifera indica* L.) cultivars in China. Food Chem. **138**, 396–405 (2013)

19. V. Eyarkai Nambi, K. Thangavel, D. Manohar Jesudas, Scientific classification of ripening period and development of colour grade chart for Indian mangoes (*Mangifera indica* L.) using multivariate cluster analysis. Sci. Hortic. **193**, 90–98 (2015)

20. A. Watanawan, C. Watanawan, J. Jarunate, Bagging 'Nam Dok Mai #4' mango during development affects color and fruit quality. Acta Hortic. **787**, 325–328 (2008)

21. V. Chonhenchob, D. Kamhangwong, J. Kruenate, K. Khongrat, N. Tangchantra, U. Wichai, S.P. Singh, Preharvest bagging with wavelength-selective materials enhances development and quality of mango (*Mangifera indica* L.) cv. Nam Dok Mai #4. J. Sci. Food Agric. **91**, 664–671 (2011)

22. S. Jha, A. Kingsly, S. Chopra, Physical and mechanical properties of mango during growth and storage for determination of maturity. J. Food Eng. **72**, 73–76 (2006)

23. Y. Fuchs, E. Pesis, G. Zauberman, Changes in amylase activity, starch and sugar contents in mango fruit pulp. Sci. Hortic. **13**, 155–160 (1980)

24. S.M. Blankenship, D.D. Ellsworth, R.L. Powell, A ripening index for banana fruit based on starch content. HortTechnology **3**, 338–339 (1993)

25. M.S. Reid, C.A.S. Padfield, C.B. Watkins, J.E. Harman, Starch iodine pattern as a maturity index for Granny Smith apples 1. Comparison with flesh firmness and soluble solid contents. N. Z. J. Agric. Res. **25**, 229–237 (1982)

26. V. Paul, R. Pandev, Role of internal atmosphere on fruit ripening and storability—a review. J. Food Sci. Technol. **51**, 1223–1250 (2014)

27. M. Castrilloo, N. Kruger, F. Whatley, Sucrose metabolism in mango fruit during ripening. Plant Sci. **84**, 45–51 (1992)

28. I. Ibarra-Garza, P. Ramos-Parra, C. Hernández-Brenes, D. Jacobo-Velázquez, Effects of postharvest ripening on the nutraceutical and physicochemical properties of mango *Mangifera indica* L. cv Keitt). Postharvest Biol. Technol. **103**, 45–54 (2015)

29. A. Medlicott, A. Thompson, Analysis of sugars and organic acids in ripening mango fruits (*Mangifera indica* L. var Keitt) by high performance liquid chromatography. J. Sci. Food Agric. **36**, 561–566 (1985)

30. N. Hubbard, D. Pharr, S. Huber, Role of sucrose phosphate synthase in sucrose biosynthesis in ripening bananas and its relationship to the respiratory climacteric. Plant Physiol. **94**, 201–208 (1990)

31. F. Wang, A.G. Smith, M.L. Brenner, Temporal and spatial expression pattern of sucrose synthase during tomato fruit development. Plant Physiol. **104**, 535–540 (1994)

32. T. Malando, R. Shewfelt, G. Ware, E. Baldwin, Sugars and acids influence flavor properties of mango (*Mangifera indica*). J. Am. Soc. Hortic. Sci. **126**, 115–121 (2001)

33. J. Cruz, C. Soares, A. Fabbri, B. Cordenunsi, S. Sabato, Effect of quarantine treatments on the carbohydrate and organic acid content of mangoes (cv. Tommy Atkins). Radiat. Phys. Chem. **81**, 1059–1063 (2012)

34. A. Medlicott, S. Reynolds, A. Thompson, Effects of temperature on the ripening of mango fruit (*Mangifera indica* L. var. Tommy Atkins). J. Sci. Food Agric. **37**, 469–474 (1986)

35. H. Palafox-Carlos, E. Yahia, M. Islas-Osuna, P. Gutierrez-Martinez, M. Robles-Sánchez, G. González-Aguilar, Effect of ripeness stage of mango fruit (*Mangifera indica* L., cv. Ataulfo) on physiological parameters and antioxidant activity. Sci. Hortic. **135**, 7–13 (2012)

36. B. Tavar, H.S. Barcia, M. Mata, Physiology of pre-cut mango II. Evolution of organic acids. Food Res. Int. **34**, 705–714 (2001)

37. J. Brecht, E. Yahia, Postharvest Physiology, in *The Mango, Botany, Production and Uses*, ed. by R.E. Litz (CABI, London, 2009), pp. 484–528